JAAS

PAPER

View Article Online
View Journal | View Issue

Cite this: J. Anal. At. Spectrom., 2017, 32, 367

Optimization of distances between the target surface and focal point on spatially confined laser-induced breakdown spectroscopy with a cylindrical cavity

Jin Guo,[a] Junfeng Shao,[a] Tingfeng Wang,[a] Changbin Zheng,[a] Anmin Chen*[bc] and Mingxing Jin*[bc]

Received 2nd November 2016
Accepted 7th December 2016

DOI: 10.1039/c6ja00396f

www.rsc.org/jaas

The spatial confinement effect in laser-induced plasma with different distances between the target surface and focal point is investigated by optical emission spectroscopy. A Nd:YAG laser is used to produce plasma from a silicon sample in air atmosphere. When the appropriate distance is selected, the duration of spectral emission enhancement is much longer, and the enhancement effect is much stronger. The phenomenon is attributed to the aspect ratio of the lateral to axial direction of the plasma plume. The plasma plume of a large aspect ratio will interact with the reflected shockwave in a long range of delay time, leading to high particle density. This provided a better understanding about the effect of the distance between the target surface and focal point, leading to better conditions for spatially confined laser-induced breakdown spectroscopy.

1 Introduction

Laser-induced breakdown spectroscopy (LIBS), which is also known as laser-induced plasma spectroscopy (LIPS), is a very promising spectral analysis technique for detecting elemental composition.[1] This technique is performed by focusing the laser beam on a small area at the surface of the specimen of interest, which is then ablated in the range from nanograms to picograms, and a plasma plume can be generated. The emission spectrum is recorded, and the neutral and ionic lines in the plasma spectroscopy are analyzed. Obviously, the intensity of spectral line is important for analysis of the sample, and determines the sensitivity and the limit of detection in LIBS.[2–4] Therefore, improving the emission intensity of LIBS technique becomes the key to the further development and application of LIBS.

With the development of a variety of laser techniques, a number of methods have been used to enhance the emission intensity of LIBS, including the use of short wavelength lasers,[5–7] double-pulse lasers,[8–10] magnetic fields,[11] spark discharges,[12,13] spatial confinement effects,[14,15] flame-enhanced LIBS,[16,17] nanoparticle-enhanced LIBS,[18,19] and resonance-enhanced LIBS.[20] In the above methods, the spatially confined LIBS shows its most advantageous aspect, the device of spatial confinement is the simplest and has least cost compared with other enhanced methods.[21] The spatial confinement increases the spectral intensity in plasma by increasing plasma temperature and electron density. The generation of plasma in air is accompanied by a shock wave. When a barrier is placed around the plasma plume, the shock wave encounters the barrier during its expansion and the shock wave will be reflected back to the plasma plume. The reflected shock wave compresses the plasma plume, resulting in the increase of the collision rate among the particles.[15,22] Therefore, the number of atoms in high-energy excited states increases, and optical emission intensity is enhanced.

In addition, many previously published papers have indicated that LIBS is relevant to the laser parameters, including the laser wavelength, pulse width, and intensity.[23–26] The properties of LIBS also depend on the laser spot size, and on the distance between the target surface and focal point. This distance has an important influence on the plasma plume expansion process because of the interaction between the plasma plume and the laser spatial energy distribution,[24,27,28] while spatially confined LIBS is directly related to the dynamics of the plasma plume.[29,30] Until now almost no studies have focused on studying the effect of the distances between the target surface and focal point in spatially confined laser-induced breakdown spectroscopy. The present work is to offer an experimental study that aims to investigate the influence of the distances between the target surface and focal point on the spectral emission intensity of

[a]State Key Laboratory of Laser Interaction with Matter and Innovation Laboratory of Electro-Optical Countermeasures Technology, Changchun Institute of Optics, Fine Mechanics and Physics, Chinese Academy of Sciences, Changchun 130033, China
[b]Institute of Atomic and Molecular Physics, Jilin University, Changchun 130012, China. E-mail: amchen@jlu.edu.cn; mxjin@jlu.edu.cn
[c]Jilin Provincial Key Laboratory of Applied Atomic and Molecular Spectroscopy (Jilin University), Changchun 130012, China

spatially confined laser-induced plasma with a cylindrical cavity. The time-resolved optical emission at different distances from a silicon surface is investigated by moving the position of the focusing lens. The results show that the distance between the target surface and focal point is found to be important for obtaining the optimal emission intensity of spatially confined LIBS. We hope that this study serves as a helpful reference for future research on LIBS.

2 Experimental setup

A schematic drawing of the experimental setup used for studying the effect of the distances between the target surface and focal point in spatially confined LIBS with a cylindrical cavity is shown in Fig. 1(a). A Nd:YAG laser system (Continuum, Surelite III) is used to generate the plasma. The output laser wavelength is 1064 nm with a repetition rate of 10 Hz. The pulse width is 10 ns. The pulsed laser is focused by using a plano-convex lens with a 10 cm focal length through a cylindrical cavity (height: 6 mm, diameter: 8 mm) to the silicon (Si⟨100⟩, MTI KJ Group, 500 ± 10 μm thickness) target surface. The cylindrical cavity is placed tightly on the surface of the Si target surface. The Si plasma is generated inside the cylindrical cavity. The Si target is located at different distances away from the focal point, as shown in Fig. 1(b). The focal point of focusing lens is at 0 mm, and the corresponding position of the target surface is in the range from 2.5 mm to 27.5 mm. To prevent over ablation, the Si target is mounted on a computer-controlled 3D motorized translation stage (Thorlabs, PT3/M-Z8) so that a new surface is exposed before the laser shot. The optical emission from the laser-induced Si plasmas is collected by using a focusing lens and dichroic mirror, and then is focused onto an optical fiber by using another lens (BK7) with a focal length of 75 mm. The optical fiber is coupled to a spectrometer (Spectra Pro 500, PI Acton, the used grating is 1200 grooves per mm). The scattered light is detected with an intensified charge-coupled device (ICCD, PIMAX4, Princeton Instruments), 1024 × 1024 pixels triggered by a photodiode. The signal of the photodiode is considered to be the zero reference time point of ICCD in this experiment. The ICCD is operated in the gated mode. The gate width is 500 ns. The spectra are averaged over 10 laser pulses to minimize the error. The whole experiment is performed in ambient air.

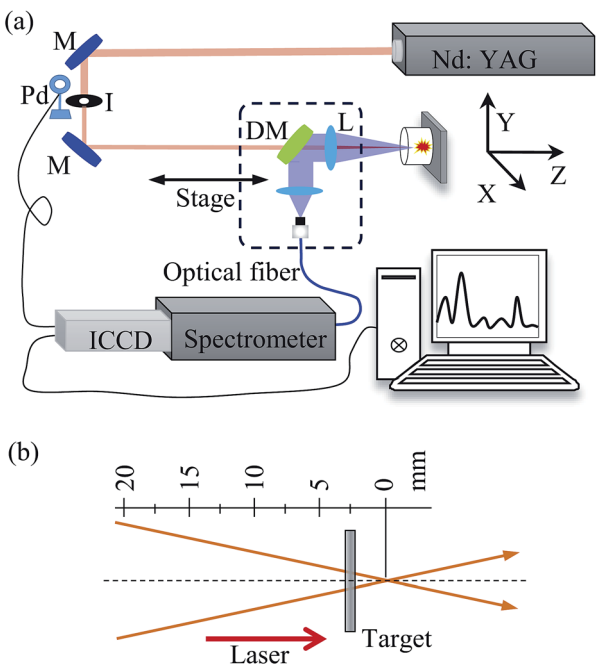

Fig. 1 (a) Schematic diagram of the experimental setup for optical emission spectroscopy (M, mirror; Pd, photodiode; I, iris; DM, dichroic mirror; L, lens; ICCD, intensified CCD). (b) Distance between the target surface and focal point.

3 Results and discussion

The time-resolved optical emission spectra of the laser-induced Si plasmas in a spectral range from 385 nm to 400 nm are recorded to demonstrate the spectral emission enhancement effect with and without the presence of a cylindrical cavity (diameter: 8 mm, height: 6 mm), as shown in Fig. 2. The

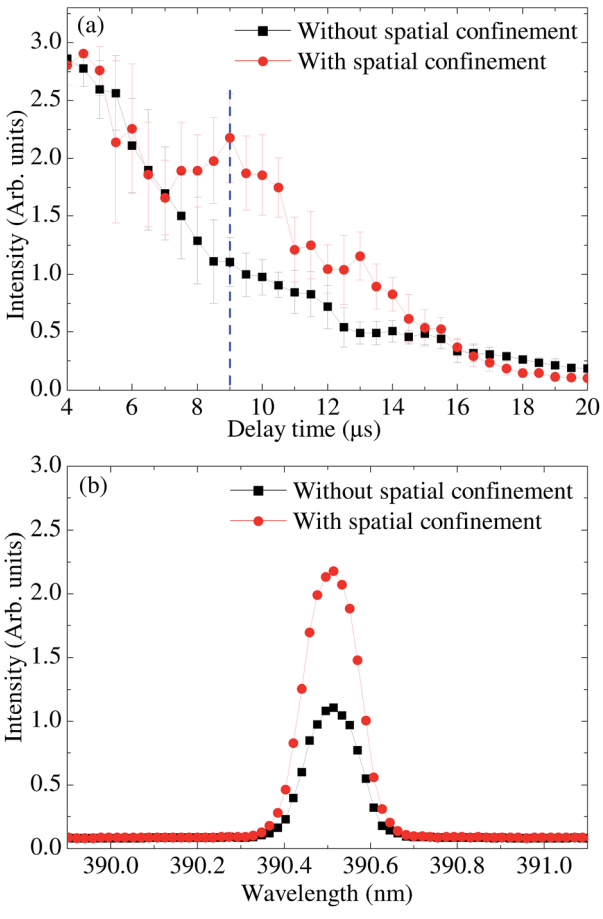

Fig. 2 Time-resolved spectroscopy of Si(I) 390.55 nm with and without the presence of a cylindrical cavity (diameter: 8 mm, height: 6 mm) at the laser energy of 33 mJ (a). Note: (b) shows the spectral intensity of selected delay time (9 μs) from (a, dashed line). The distance of the focal point is 8.75 mm.

measured spectral line that is collected with the BK7 lenses is that of Si(I) at 390.55 nm from the $3s^2 3p^2(^1S_0) \leftarrow 3s^2 2p4s(^1P_1)$ transition. As can be seen in Fig. 2(a), the emission intensity of the Si(I) line without the presence of the cylindrical spatially confined cavity decays monotonously with the increase of delay time. However, as the cylindrical cavity is used to confine the plasma, the emission intensity of the Si(I) line is enhanced during the period of delay time from 7 μs to 15 μs. In order to better compare the enhancement of the spectral line, we select the typical delay time (9 μs) from Fig. 2(a). As shown in Fig. 2(b), the emission intensity of Si(I) line is enhanced obviously, the enhanced factor is approximately 2. The baseline of the spectrum is almost unchanged. So, the signal-to-background ratio is also improved. When the delay time lasted for several microseconds, the plasma in this time period emits sharp atomic spectral lines with a negligibly low background (continuous spectrum) and highly favorable characteristics for elemental analysis. Additionally the linear relationship between the emission line intensities and the contents of associated elements in the sample has also made it uniquely suitable for quantitative analysis.[31–33]

At the local thermodynamic equilibrium, the emission intensity for spectroscopy, corresponding to a transition from level k to level i, is given by $I_\lambda = F_{exp}N(A_{ki}g_k/\lambda U(T_p))(\exp(-E_k/(k_bT_p)))$.[7,34,35] Here, A_{ki} is the transition probability, g_k and E_k are the degeneracy and the energy of the upper level k, $U(T_p)$ is the partition function, λ is the emission wavelength, k_b is the Boltzmann constant, N is the total number density of a species at a given ionization stage, T_p is the plasma temperature, and F_{exp} is the experimental coefficient with respect to the efficiency of the optical detection system. According to this equation, for the same spectral line, most of the parameters (A_{ki}, g_k, E_k, $U(T_p)$, λ, k_b, and F_{exp}) are the same. The only possible differences are thus in N and T_p. Therefore, the spectral enhancement is based on the increase in the plasma temperature and particle density caused by spatial confinement. A cylindrical cavity is used to confine the laser-induced plasma in air, this physical process is accompanied by the generation of a shock wave because of the initial explosive pressure. The shock wave comes from the rapid increase in the ambient air pressure. The expansion speed of a shock wave is typically much faster than the speed of sound, so the wall of the spatial confinement cavity is equivalent to an obstacle.[36] If the shock wave in the process of expansion encounters the obstacle, the shock wave will be reflected back to the region of the plasma plume. The reflected shockwave compresses the plasma plume and confines it within a small area. This increases the plasma temperature and particle density in its original region.[37,38] The intensity of the spectral line in LIBS is enhanced by using the spatially confined cavity.

The characteristics of LIBS are highly dependent on the distance between the target surface and focal point. The distribution of emission intensity produced by the laser-induced Si plasmas for the spectral line of Si(I) 390.55 nm with the delay time and the distance between the target surface and focal point is shown in Fig. 3. The laser energy is 33 mJ. The distribution of the emission intensity is obtained by moving the position of the focusing lens and changing the delay time of

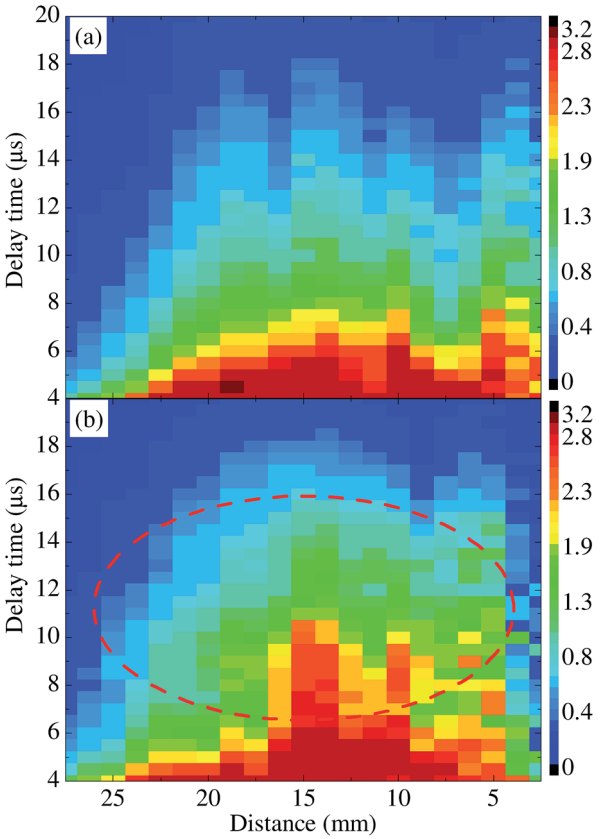

Fig. 3 Time-resolved spectroscopy of Si(I) 390.55 nm without spatial confinement (a) and with spatial confinement (b) for different focal point distances. Laser energy is 33 mJ.

ICCD. And, in order to avoid air breakdown, we only measure the distances from the focal point to the opposite direction of laser (as shown in Fig. 1(b)). These values represent the focal point inside the target. In the processes of the experiment, the distance between the target surface and focal point is less than 7.5 mm, the air breakdown may occur at a certain probability. As the distance is greater than 25 mm, the decay of emission intensity is very quick. As seen from this Fig. 3(a), the time-resolved optical emission of the Si(I) line is sensitive to the different distances between the target surface and focal point. The emission intensity of Si(I) first begins to rise with the increase of the distance, and then drops. At a distance of 15 mm, the emission intensity is strong compared with the other distances. It is well known that, in nanosecond pulse laser ablation, the leading edge of a nanosecond laser pulse is used to ablate the target and produce a plasma on the target surface, while the trailing edge of the nanosecond laser pulse will interact with the produced plasma and heat the plasma rather than interacting with the target.[24,28] When the focusing lens is used to change the distance between the target surface and focal point, the spot size at the target surface will be increased or decreased.[39] When the distance is shorter (the spot size is smaller), due to the smaller cone angle of the laser beam, the plasma absorption will be localized near the vicinity of the central axis. When the focusing lens is away from the focal point

(the spot size is larger), the laser cone angle will be larger, and hence, the trailing edge of the nanosecond laser pulse will be efficiently distributed among the entire plasma front. This provides a better coupling between the laser and plasma, leading to better heating conditions for the plasma produced by the leading edge of the nanosecond laser.[24,39] The distance is greater than 25 mm (Fig. 3(a)), the focusing lens is so near that the produced plasma is very weak.

As can be seen in Fig. 3, when the cylindrical cavity is used to confine the plasma plume (Fig. 3(b)), the emission intensity of Si(I) is higher than that of laser-induced Si plasma without the spatial confinement. A dotted ellipse on the enhanced area is shown in Fig. 3(b). The cylindrical cavity causes the plasma spectroscopy to be stronger in a specific period of delay time. Also, the spectral emission enhancement of the Si(I) is found to depend on the distance between the target surface and focal point. Different sample positions (the distance) can obviously affect the enhancement of the emission intensity. Therefore, the emission intensity of the plasma generated from spatially confined laser-induced Si in air should be further discussed.

To aid the understanding of the detailed information about the effect of the distance between the target surface and focal point on the spatially confined LIBS, time-resolved spectroscopy of Si(I) 390.55 nm selected from Fig. 3 at the different distances is shown in Fig. 4. As seen from Fig. 4(a), at the distance of 22.5 mm, the time-resolved spectroscopy with the spatial confinement shows the enhanced optical emission in the range of delay time from 7 μs to 13 μs compared with the time-resolved spectroscopy without the spatial confinement. When the distance decreases from 22.5 mm to 20 mm (Fig. 4(a–c)), the enhancement effect gradually increases. At the distances of 15 mm and 13.75 mm (Fig. 4(d and e)), the enhancement effect is the best. The range of delay time of enhanced optical emission extends to both sides from 5 μs to 18 μs. Also the spectral emission intensity increases obviously compared with that in the distances from 22.5 mm to 20 mm (Fig. 4(a–c)). When continued to decrease the distance, the enhanced time range reduces and emission intensity decreases. When the distance is 7.5 mm (Fig. 4(i)), the error of spectral emission intensity is larger than that in Fig. 4(a–h) due to the presence of a laser-induced air breakdown at a certain probability. And, the

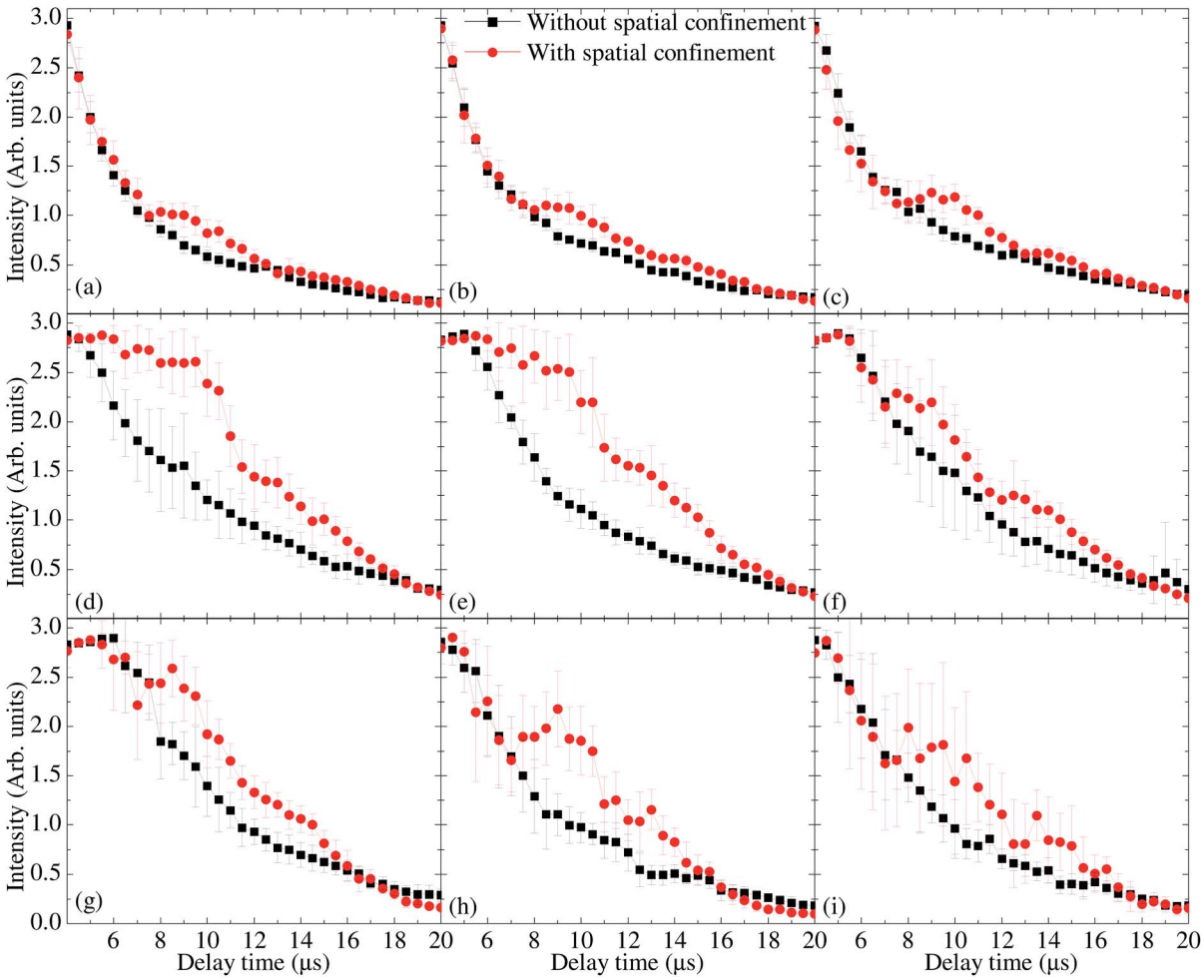

Fig. 4 Time-resolved spectroscopy of Si(I) 390.55 nm with and without the presence of a cylindrical cavity (diameter: 8 mm, height: 6 mm) at different focal point distances selected from Fig. 3. The distances are 22.5 mm (a), 21.25 mm (b), 20 mm (c), 15 mm (d), 13.75 mm (e), 12.5 mm (f), 10 mm (g), 8.75 mm (h), and 7.5 mm (i).

probability of air breakdown with the cylindrical cavity is larger than that without the cylindrical cavity. This can also be observed at the distances of 3.75 mm and 2.5 mm in Fig. 3. When laser-induced air breakdown takes place, the spectral emission intensity of laser-induced Si plasma is significantly reduced due to the plasma shielding effects.[27] The increased probability of laser-induced air breakdown occurring with the cylindrical cavity may be attributed to the scattered laser-induced electron emission from the metal wall of the cylindrical cavity. However, the contribution of the scattered laser-induced electron emission is not well understood and remains an interesting issue to be investigated in future.

Fig. 5 shows the distribution of the enhancement ratio of Si(I) 390.55 nm with the focal point distances and delay times. The enhancement ratio of the emission intensity is calculated from the results in Fig. 4 by dividing the emission intensities with the cylindrical cavity by the emission intensity without the spatial confinement. As seen from this figure, in the range of distance from 12.5 mm to 17.5 mm, the enhancement ratio is higher compared with other distance. At the distance of 15.0 mm, the enhancement ratio is the maximum, and the spectral emission is also the strongest (in Fig. 3(b)). Therefore, we can optimize the emission intensity of LIBS with the spatial confinement by varying the distances between the target surface and focal point.

For the optimized distance in spatially confined LIBS, the dynamics of the plasma plume is dependent on the spot size at the surface of the target. At the same laser energy, the plasma plume behavior can be quite different, which means that the laser energy and spot size have differing degrees of influence on the development of laser-induced plasma.[39,40] Li *et al.* investigated the influence of the spot size on the expansion dynamics of nanosecond laser-induced copper plasmas in air atmosphere.[27] The results showed that, when the laser energy was fixed, the spot size strongly influenced the dynamics of the laser-induced plasma; a large spot size resulted in a hemispherical structure and a small spot size in a stream-like shape of the plasma plume. The structural schematic diagram of the plasma plume is shown in Fig. 6. In other words, for a long distance between the target surface and focal point (large spot size), the laser-induced plasma plume expands in both lateral and axial directions with a hemispherical structure, as seen in Fig. 6(a). The aspect ratio of the lateral to axial direction is large. Therefore, the duration of interaction between the shock wave reflected by the wall of the cylindrical cavity and the plasma plume in the lateral direction will be extended, and the particle density in the plasma plume will be higher, resulting in stronger spectral emission. As shown in Fig. 4(d), the duration of spectral emission enhancement is much longer than that in Fig. 4(e–i). When the distance between the target surface and focal point decreases, the spot size decreases and the aspect ratio of the lateral to axial direction decreases. The small spot size gives the plasma plume a narrow cylindrical structure, as seen in Fig. 6(b). In this case, the reflected shock wave compresses the plasma plume in a shorter time period, thus the time of interaction is reduced. And, the particle density is low compared with the case of the large aspect ratio in Fig. 6(a). Finally, as the position is far away from the focal point, the laser-induced plasma becomes weaker, the accompanied shock wave weakens due to the weak interaction between the laser and target. The enhancement of spectral emission is not obvious. Therefore, we can optimize the emission intensity of spatially confined LIBS by varying the distance between the target surface and focal point.

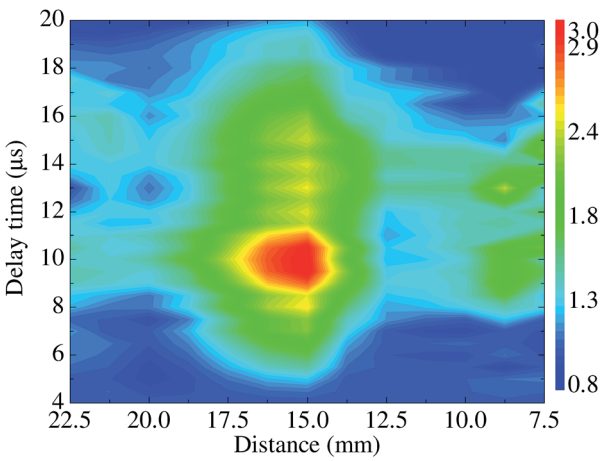

Fig. 5 Distribution of enhancement ratio with the focal point distances and delay times from Fig. 4.

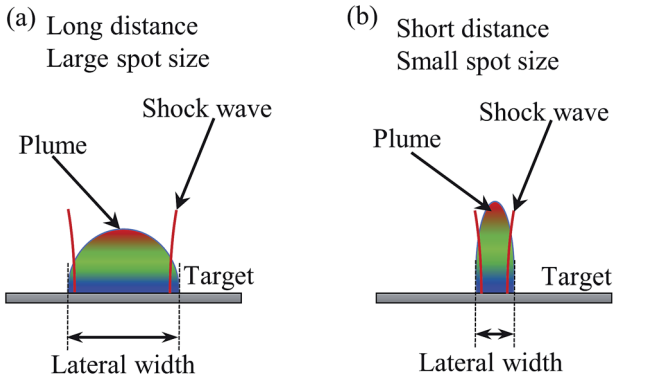

Fig. 6 Schematic diagram of the interaction between the reflected shock wave and plasma plume. (a) Hemispherical structure at the large spot size. (b) Cylindrical structure at the small spot size.

4 Conclusion

In conclusion, we utilized a cylindrical cavity of 8 mm diameter and 6 mm height to confine laser-induced Si plasmas with different distances between the target surface and focal point in air atmosphere. The recorded spectral line is Si(I) at 390.55 nm. The characteristics of time-resolved spectroscopy are highly dependent on the distance between the target surface and focal point. When the cylindrical cavity is used to confine the plasma plume, the emission intensity of Si(I) is higher than that of laser-induced Si plasma without the spatial confinement in a specific period of delay time. By selecting an appropriate distance

between the target surface and focal point, the enhancement effect can be optimized. The optimized distance can cause the spectral emission to be stronger and extend the duration of interaction between the reflected shock wave and plasma plume. We hope that this study serves as a helpful reference for future research on spatially confined LIBS.

Acknowledgements

This work was supported by the National Natural Science Foundation of China (11674128, 11474129 and 11504129); the Program 973 (2013CB922200); the China Postdoctoral Science Foundation (2014M551169).

References

1 A. W. Miziolek, V. Palleschi and I. Schechter, *Laser-induced breakdown spectroscopy*, Cambridge University Press, 2006.
2 R. Noll, *Laser-induced breakdown spectroscopy*, Springer, 2012.
3 A. M. Rubenchik, M. P. Fedoruk and S. K. Turitsyn, *Light: Sci. Appl.*, 2014, **3**, e159.
4 R. Kammel, R. Ackermann, J. Thomas, J. Götte, S. Skupin, A. Tünnermann and S. Nolte, *Light: Sci. Appl.*, 2014, **3**, e169.
5 X. Li, Z. Wang, Y. Fu, Z. Li and W. Ni, *Plasma Sci. Technol.*, 2015, **17**, 621.
6 Y. Wang, A. Chen, S. Li, L. Sui, D. Liu, D. Tian, Y. Jiang and M. Jin, *J. Anal. At. Spectrom.*, 2016, **31**, 497–505.
7 A. Chen, Y. Wang, L. Sui, S. Li, S. Li, D. Liu, Y. Jiang and M. Jin, *Opt. Express*, 2015, **23**, 24648–24656.
8 F.-F. Chen, X.-J. Su and W.-D. Zhou, *Frontiers of Physics*, 2015, **10**, 1–8.
9 A. Chen, S. Li, S. Li, Y. Jiang, J. Shao, T. Wang, X. Huang, M. Jin and D. Ding, *Phys. Plasmas*, 2013, **20**, 103110.
10 H. Qi, S. Li, Y. Qi, A. Chen, Z. Hu, X. Huang, M. Jin and D. Ding, *J. Anal. At. Spectrom.*, 2014, **29**, 1105–1111.
11 P. K. Pandey and R. K. Thareja, *Phys. Plasmas*, 2013, **20**, 022117.
12 W. D. Zhou, X. J. Su, H. G. Qian, K. X. Li, X. F. Li, Y. L. Yu and Z. J. Ren, *J. Anal. At. Spectrom.*, 2013, **28**, 702–710.
13 O. A. Nassef and H. E. Elsayed-Ali, *Spectrochim. Acta, Part B*, 2005, **60**, 1564–1572.
14 Z. Y. Hou, Z. Wang, J. M. Liu, W. D. Ni and Z. Li, *Opt. Express*, 2013, **21**, 15974–15979.
15 A. M. Popov, F. Colao and R. Fantoni, *J. Anal. At. Spectrom.*, 2010, **25**, 837–848.
16 L. Liu, S. Li, X. N. He, X. Huang, C. F. Zhang, L. S. Fan, M. X. Wang, Y. S. Zhou, K. Chen, L. Jiang, J. F. Silvain and Y. F. Lu, *Opt. Express*, 2014, **22**, 7686–7693.
17 L. Liu, X. Huang, S. Li, Y. Lu, K. Chen, L. Jiang, J. F. Silvain and Y. F. Lu, *Opt. Express*, 2015, **23**, 15047–15056.
18 A. De Giacomo, R. Gaudiuso, C. Koral, M. Dell'Aglio and O. De Pascale, *Anal. Chem.*, 2013, **85**, 10180–10187.
19 A. Chen, Y. Jiang, T. Wang, J. Shao and M. Jin, *Phys. Plasmas*, 2015, **22**, 033301.
20 C. Goueguel, S. Laville, F. Vidal, M. Sabsabi and M. Chaker, *J. Anal. At. Spectrom.*, 2010, **25**, 635–644.
21 D. Ding, P. Liang, J. Wu, N. Xu, Z. Ying and J. Sun, *Spectrochim. Acta, Part B*, 2013, **79–80**, 44–50.
22 X. K. Shen, J. Sun, H. Ling and Y. F. Lu, *Appl. Phys. Lett.*, 2007, **91**, 081501.
23 S. Harilal, *J. Appl. Phys.*, 2007, **102**, 123306.
24 S. Harilal, R. Coons, P. Hough and A. Hassanein, *Appl. Phys. Lett.*, 2009, **95**, 221501.
25 J. T. Schiffern, D. W. Doerr and D. R. Alexander, *Spectrochim. Acta, Part B*, 2007, **62**, 1412–1418.
26 Y. Lu, V. Zorba, X. Mao, R. Zheng and R. E. Russo, *J. Anal. At. Spectrom.*, 2013, **28**, 743–748.
27 X. Li, W. Wei, J. Wu, S. Jia and A. Qiu, *J. Appl. Phys.*, 2013, **113**, 243304.
28 S. Harilal, P. Diwakar, M. Polek and M. Phillips, *Opt. Express*, 2015, **23**, 15608–15615.
29 X. Shen, J. Sun, H. Ling and Y. Lu, *J. Appl. Phys.*, 2007, **102**, 093301.
30 L. Guo, W. Hu, B. Zhang, X. He, C. Li, Y. Zhou, Z. Cai, X. Zeng and Y. Lu, *Opt. Express*, 2011, **19**, 14067–14075.
31 K. Kagawa, M. Ohtani, S. Yokoi and S. Nakajima, *Spectrochim. Acta, Part B*, 1984, **39**, 525–536.
32 H. Kurniawan, T. J. Lie, K. Kagawa and M. O. Tjia, *Spectrochim. Acta, Part B*, 2000, **55**, 839–848.
33 K. Kagawa, Y. Matsuda, S. Yokoi and S. Nakajima, *J. Anal. At. Spectrom.*, 1988, **3**, 415–419.
34 J. Guo, T. Wang, J. Shao, T. Sun, R. Wang, A. Chen, Z. Hu, M. Jin and D. Ding, *Opt. Commun.*, 2012, **285**, 1895–1899.
35 M. L. Shah, A. K. Pulhani, B. M. Suri and G. P. Gupta, *Plasma Sci. Technol.*, 2013, **15**, 546–551.
36 Y. Wang, A. Chen, L. Sui, S. Li, X. Wang, Y. Jiang, X. Huang and M. Jin, *J. Anal. At. Spectrom.*, 2016, **31**, 1974–1977.
37 X. Gao, L. Liu, C. Song and J. Lin, *J. Phys. D: Appl. Phys.*, 2015, **48**, 175205.
38 Y. Fu, Z. Hou and Z. Wang, *Opt. Express*, 2016, **24**, 3055.
39 E. Voropay and K. Ermalitskaia, *Eur. Phys. J. D*, 2011, **64**, 453–458.
40 C. Diao, C. Chen, B. Man, C. Wang and H. Fu, *Eur. Phys. J. D*, 2011, **63**, 123–128.

